EARTHQUAKE ENGINEERING AND STRUCTURAL DYNAMICS
Earthquake Engng Struct. Dyn. 2011; **40**:119–133
Published online 22 March 2010 in Wiley Online Library (wileyonlinelibrary.com). DOI: 10.1002/eqe.1004

Simplified analysis of mid-story seismically isolated buildings

Shiang-Jung Wang[1,2,‡,**], Kuo-Chun Chang[1,2,*,†,§,¶], Jenn-Shin Hwang[2,3,§,‖] and Bo-Han Lee[1,**]

[1]*Department of Civil Engineering, National Taiwan University, Taipei, Taiwan*
[2]*National Center for Research on Earthquake Engineering, Taipei, Taiwan*
[3]*Department of Construction Engineering, National Taiwan University of Science and Technology, Taipei, Taiwan*

SUMMARY

The mid-story isolation design method is recently gaining popularity for the seismic protective design of buildings located in the areas of high population. In a mid-story isolated building, the isolation system is incorporated into the mid-story rather than the base of the building. In this paper, the dynamic characteristics and seismic responses of mid-story isolated buildings are investigated using a simplified three-lumped-mass structural model for which equivalent linear properties are formulated. From the parametric study, it is found that the nominal frequencies of the superstructure and the substructure, respectively, above and below the isolation system have significant influences on the isolation frequency and equivalent damping ratio of a mid-story isolated building. Moreover, the mass and stiffness of the substructure are of greater significance than the superstructure in affecting the dynamic characteristics of the isolated building. Besides, based on the response spectrum analysis, it is noted that the higher mode responses may contribute significantly to the story shear force of the substructure. Consequently, the equivalent lateral force procedure of design codes should carefully include the effects of higher modes. Copyright © 2010 John Wiley & Sons, Ltd.

Received 30 July 2009; Revised 18 January 2010; Accepted 27 January 2010

KEY WORDS: mid-story isolation; seismic design; structural control; base isolation

INTRODUCTION

The excellent performance of seismically isolated buildings during the 1994 Northridge earthquake and 1995 Kobe earthquake has encouraged the adoption of seismic isolation design for structural protection in the past two decades [1–6]. The application of seismic isolation design in Taiwan has also been extensive after the 1999 Chi-Chi earthquake [7]. The seismic isolation design guidelines have correspondingly been refined [8–11]. Among the increasing practical applications, the mid-story isolation design, in which the isolation system is typically installed on the top of the first story of a building, is recently gaining popularity because it can satisfy both architectural concerns of aesthetics and functionality. More importantly, it can enhance the construction feasibility at highly populated areas where installing the isolation system beneath the base of a building is extremely

*Correspondence to: Kuo-Chun Chang, National Center for Research on Earthquake Engineering, Taipei, Taiwan.
†E-mail: kcchang@ncree.org.tw
‡Assistant Researcher.
§Professor.
¶Director General.
‖Deputy Director General.
**Ph.D. Student.

Contract/grant sponsor: National Center for Research on Earthquake Engineering of Taiwan

difficult if the building separation and property line are of particular concerns. The effectiveness of mid-story isolation design in reducing seismic demand on the superstructure above the isolation system has been numerically proved [12, 13]. A simplified two-lumped-mass structural model has been proposed to numerically investigate the seismic responses of mid-story isolated structures [14, 15]. In the simplified structural model, the superstructure above the isolation system is ideally assumed to behave as a rigid body. Some simplified structural models [16, 17] have also been proposed to predict the seismic responses of mid-story isolated structures. Static and dynamic analyses for mid-story isolated buildings with and without velocity-dependent dampers have been reported [18].

The existing seismic isolation design guidelines are tailored for base-isolated buildings rather than for mid-story isolated buildings. Little has been documented for the design of mid-story isolated structures. In current practice, the preliminary design of mid-story isolated buildings usually follows the equivalent lateral force procedure provided for base-isolated buildings, assuming that the substructure is sufficiently stiff or rigid. However, the dynamic behavior of a mid-story isolated structure and a base-isolated structure may not be identical since the seismic responses of a mid-story isolated building may be significantly affected by the flexibility of the substructure, e.g. the first story. Furthermore, the interaction between the superstructure and the substructure may not be negligible. Therefore, a non-linear response history analysis for the final design check should be required in current practice.

The adoption of mid-story isolation design should consider at least the following issues (1) the seismic performance of the superstructure of a mid-story isolated building is warranted to be as good as that of a base-isolated building; (2) the fundamental (or isolated) period and effective damping ratio of the isolated building should be accurately captured if the equivalent lateral force procedure is to be applied; (3) possible damages to the substructure should be prevented; and (4) special attention has to be paid to the design of the substructure (first story) such that the unexpected seismic responses due to the coupling of higher modes can be avoided [19, 20]. In order to gain insight into the seismic responses of mid-story isolated buildings, this study aims to investigate the dynamic characteristics and seismic behavior of mid-story isolated buildings represented by a simplified three-lumped-mass structural model. The dynamic characteristics attributed to the substructure and superstructure are considered comprehensively in the novel structural model such that both the effects of the substructure and superstructure on the modal quantities and dynamic responses of a mid-story isolated building can be realized better. The corresponding equivalent linear properties of the simplified model are formulated and the effects of various parameters, including masses and vibration frequencies of the superstructure and substructure on the dynamic characteristics of mid-story isolated structures, are examined. Furthermore, the response spectrum analysis is conducted to investigate the significances of all vibration modes on the seismic responses of mid-story isolated buildings.

EQUIVALENT LINEAR CHARACTERISTICS

Referring to the simplified two-lumped-mass structural model for base-isolated buildings proposed by Kelly [21, 22] as given in Figure 1(a), a mid-story isolated building may be represented by a

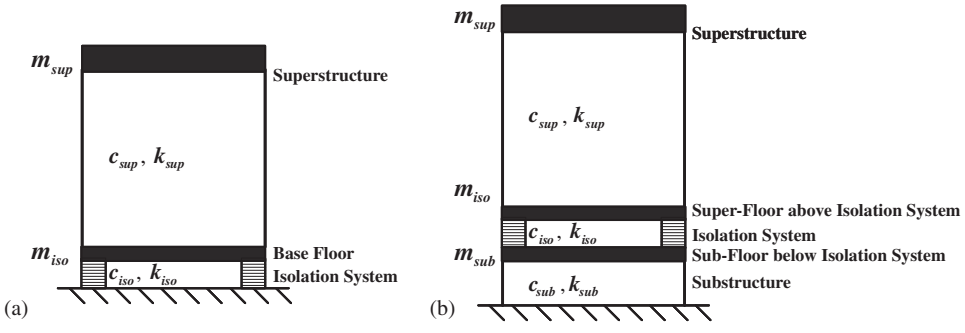

Figure 1. Simplified models for base-isolated and mid-story isolated buildings: (a) Two-lumped-mass structural model and (b) three-lumped-mass structural model.

DOI: 10.1002/eqe

simplified three-lumped-mass structural model, composed of the superstructure, isolation system and substructure, as shown in Figure 1(b). All structural elements, except the isolation system of the model, are assumed to remain elastic under earthquake excitations. The hysteretic behavior of seismic isolation system is represented by an equivalent linear model composed of effective stiffness and equivalent damping ratio [21, 22]. It should be noted that, employing the simplified model, the effects arising from the flexibility of foundation and soil–structure interaction are excluded in the study. The equation of motion corresponding to the simplified three-lumped-mass structural model is written in terms of story drifts

$$\begin{aligned}
&\begin{bmatrix} m_{\text{sub}} & 0 & 0 \\ m_{\text{iso}} & m_{\text{iso}} & 0 \\ m_{\text{sup}} & m_{\text{sup}} & m_{\text{sup}} \end{bmatrix} \begin{Bmatrix} \ddot{v}_{\text{sub}} \\ \ddot{v}_{\text{iso}} \\ \ddot{v}_{\text{sup}} \end{Bmatrix} + \begin{bmatrix} c_{\text{sub}} & -c_{\text{iso}} & 0 \\ 0 & c_{\text{iso}} & -c_{\text{sup}} \\ 0 & 0 & c_{\text{sup}} \end{bmatrix} \begin{Bmatrix} \dot{v}_{\text{sub}} \\ \dot{v}_{\text{iso}} \\ \dot{v}_{\text{sup}} \end{Bmatrix} \\
&\quad + \begin{bmatrix} k_{\text{sub}} & -k_{\text{iso}} & 0 \\ 0 & k_{\text{iso}} & -k_{\text{sup}} \\ 0 & 0 & k_{\text{sup}} \end{bmatrix} \begin{Bmatrix} v_{\text{sub}} \\ v_{\text{iso}} \\ v_{\text{sup}} \end{Bmatrix} \\
&\quad = -\begin{bmatrix} m_{\text{sub}} & 0 & 0 \\ 0 & m_{\text{iso}} & 0 \\ 0 & 0 & m_{\text{sup}} \end{bmatrix} \begin{Bmatrix} 1 \\ 1 \\ 1 \end{Bmatrix} \ddot{u}_{\text{g}},
\end{aligned} \tag{1}$$

where v_{sub}, v_{iso} and v_{sup} are the inter-story displacements (story drifts) of the substructure, isolation layer and superstructure, respectively; $\ddot{u}_{\text{g}}$ is the ground acceleration; m_{sub}, m_{iso} and m_{sup} are the seismic reactive masses of the substructure (or sub-floor), isolation layer (or super-floor) and superstructure, respectively; k_{sub} and k_{sup} are correspondingly the elastic lateral stiffnesses of the substructure and superstructure; k_{iso} is the effective lateral stiffness of the isolation system; c_{sub} and c_{sup}, respectively, the viscous damping coefficients of the substructure and superstructure; and c_{iso} is the equivalent viscous damping coefficient of the isolation system. Defining the mass ratios $r_{\text{sub}} = m_{\text{sub}}/m_{\text{iso}}$ and $r_{\text{sup}} = m_{\text{sup}}/m_{\text{iso}}$, the mass ratios r_1, r_2 and r_3 can be expressed as follows:

$$r_1 = \frac{m_{\text{iso}} + m_{\text{sup}}}{m_{\text{sub}} + m_{\text{iso}} + m_{\text{sup}}} = \frac{1 + r_{\text{sup}}}{1 + r_{\text{sub}} + r_{\text{sup}}}, \tag{2}$$

$$r_2 = \frac{m_{\text{sup}}}{m_{\text{iso}} + m_{\text{sup}}} = \frac{r_{\text{sup}}}{1 + r_{\text{sup}}}, \tag{3}$$

$$r_3 = r_1 r_2 = \frac{m_{\text{sup}}}{m_{\text{sub}} + m_{\text{iso}} + m_{\text{sup}}} = \frac{r_{\text{sup}}}{1 + r_{\text{sub}} + r_{\text{sup}}}. \tag{4}$$

From Equations (2), (3) and (4), it is realized that the mass ratios r_1, r_2 and r_3 are all less than one. The 'nominal frequencies' [21, 22] of the substructure, isolation layer and superstructure are defined as follows:

$$\begin{aligned}
\omega_{\text{sub}} &= \sqrt{\frac{k_{\text{sub}}}{m_{\text{sub}}}}, \\
\omega_{\text{sub}}^{*} &= \sqrt{\frac{k_{\text{sub}}}{m_{\text{sub}} + m_{\text{iso}} + m_{\text{sup}}}} = \omega_{\text{sub}} \sqrt{\frac{r_{\text{sub}}}{1 + r_{\text{sub}} + r_{\text{sup}}}} = \omega_{\text{sub}} \sqrt{1 - r_1}, \\
\omega_{\text{iso}} &= \sqrt{\frac{k_{\text{iso}}}{m_{\text{iso}} + m_{\text{sup}}}}, \\
\omega_{\text{sup}} &= \sqrt{\frac{k_{\text{sup}}}{m_{\text{sup}}}}.
\end{aligned} \tag{5}$$

DOI: 10.1002/eqe

The component damping ratios ξ_{sub}, ξ_{iso} and ξ_{sup} are expressed as follows:

$$\xi_{\text{sub}} = \frac{c_{\text{sub}}}{2\omega^*_{\text{sub}}(m_{\text{sub}}+m_{\text{iso}}+m_{\text{sup}})} = \frac{c_{\text{sub}}}{2\omega^*_{\text{sub}}m_{\text{sub}}}\left(\frac{r_{\text{sub}}}{1+r_{\text{sub}}+r_{\text{sup}}}\right) = \frac{c_{\text{sub}}}{2\omega_{\text{sub}}m_{\text{sub}}}\sqrt{1-r_1}, \quad (6)$$

$$\xi_{\text{iso}} = \frac{c_{\text{iso}}}{2\omega_{\text{iso}}(m_{\text{iso}}+m_{\text{sup}})} = \frac{c_{\text{iso}}}{2\omega_{\text{iso}}m_{\text{iso}}(1+r_{\text{sup}})}, \quad (7)$$

$$\xi_{\text{sup}} = \frac{c_{\text{sup}}}{2\omega_{\text{sup}}m_{\text{sup}}}, \quad (8)$$

where ξ_{sub} and ξ_{sup} are the viscous damping ratios of the substructure and superstructure, respectively; and ξ_{iso} is the equivalent viscous damping ratio of the isolation system. With the above-defined parameters, Equation (1) can be rewritten as follows:

$$\begin{bmatrix} 1 & r_1 & r_1r_2 \\ 1 & 1 & r_2 \\ 1 & 1 & 1 \end{bmatrix} \begin{Bmatrix} \ddot{v}_{\text{sub}} \\ \ddot{v}_{\text{iso}} \\ \ddot{v}_{\text{sup}} \end{Bmatrix} + \begin{bmatrix} 2\omega_{\text{sub}}\sqrt{1-r_1}\xi_{\text{sub}} & 0 & 0 \\ 0 & 2\omega_{\text{iso}}\xi_{\text{iso}} & 0 \\ 0 & 0 & 2\omega_{\text{sup}}\xi_{\text{sup}} \end{bmatrix} \begin{Bmatrix} \dot{v}_{\text{sub}} \\ \dot{v}_{\text{iso}} \\ \dot{v}_{\text{sup}} \end{Bmatrix}$$
$$+ \begin{bmatrix} \omega^2_{\text{sub}}(1-r_1) & 0 & 0 \\ 0 & \omega^2_{\text{iso}} & 0 \\ 0 & 0 & \omega^2_{\text{sup}} \end{bmatrix} \begin{Bmatrix} v_{\text{sub}} \\ v_{\text{iso}} \\ v_{\text{sup}} \end{Bmatrix} = -\begin{bmatrix} 1 & r_1 & r_1r_2 \\ 1 & 1 & r_2 \\ 1 & 1 & 1 \end{bmatrix} \begin{Bmatrix} 1 \\ 0 \\ 0 \end{Bmatrix} \ddot{u}_g. \quad (9)$$

Solving the eigenvalue problem of Equation (9), the characteristic equation is obtained as follows:

$$\lambda^3 + a\lambda^2 + b\lambda + c = 0, \quad (10)$$

where a, b and c are given by

$$\begin{aligned} a &= -\left(\frac{\omega^2_{\text{sub}}(1-r_1)(1-r_2)+\omega^2_{\text{iso}}(1-r_1r_2)+\omega^2_{\text{sup}}(1-r_1)}{(1-r_1)(1-r_2)}\right), \\ b &= \frac{\omega^2_{\text{sub}}\omega^2_{\text{iso}}(1-r_1)+\omega^2_{\text{sub}}\omega^2_{\text{sup}}(1-r_1)+\omega^2_{\text{iso}}\omega^2_{\text{sup}}}{(1-r_1)(1-r_2)}, \\ c &= -\left(\frac{\omega^2_{\text{sub}}\omega^2_{\text{iso}}\omega^2_{\text{sup}}}{1-r_2}\right). \end{aligned} \quad (11)$$

The mode shape vectors are determined in the form of

$$\{\phi_n\} = \begin{Bmatrix} (\phi_{\text{sub}})_n \\ (\phi_{\text{iso}})_n \\ (\phi_{\text{sup}})_n \end{Bmatrix} = \begin{Bmatrix} 1 \\ \dfrac{(1-r_1)(\omega^2_{\text{sub}}-\omega^2_n)}{r_1\omega^2_{\text{iso}}} \\ \dfrac{(1-r_1)(\omega^2_{\text{sub}}-\omega^2_n)}{r_1(\omega^2_{\text{sup}}-(1-r_2)\omega^2_n)} \end{Bmatrix} \qquad n=1,2,3, \quad (12)$$

where ω_n is the modal natural frequency of the nth vibration mode; $(\phi_{\text{sub}})_n$, $(\phi_{\text{iso}})_n$ and $(\phi_{\text{sup}})_n$ are the nth mode shapes of story drifts of the substructure, isolation layer and superstructure, respectively.

The fundamental (or isolated) modal natural frequency ω_1 may be very close to the isolated frequency ω_{iso}, and is well separated from the residual modal natural frequencies if the elastic lateral stiffnesses of the substructure and superstructure are much greater than the effective lateral stiffness of the isolation system. Defining $\varepsilon_1 = \omega^2_{\text{iso}}/\omega^2_{\text{sub}}$ and $\varepsilon_2 = \omega^2_{\text{iso}}/\omega^2_{\text{sup}}$ and assuming that

DOI: 10.1002/eqe

ε_1 and ε_2 are of an order equal to or less than 10^{-1}, the first mode shape of story drifts can be approximated by substituting ω_{iso} for ω_1. Employing Equations (2) and (3), the first mode shape of story drifts is obtained from Equation (12) as follows:

$$\begin{Bmatrix} (\phi_{sub})_1 \\ (\phi_{iso})_1 \\ (\phi_{sup})_1 \end{Bmatrix} = \begin{Bmatrix} 1 \\ \dfrac{(1-r_1)(1-\varepsilon_1)}{r_1\varepsilon_1} \\ \dfrac{(1-r_1)\omega_{sub}^2(1-\varepsilon_1)}{r_1\omega_{sup}^2(1-(1-r_2)\varepsilon_2)} \end{Bmatrix} = \begin{Bmatrix} 1 \\ \dfrac{r_{sub}\omega_{sub}^2}{(1+r_{sup})\omega_{iso}^2} \\ \dfrac{r_{sub}\omega_{sub}^2}{(1+r_{sup})\omega_{sup}^2} \end{Bmatrix}, \tag{13}$$

where $(\phi_{sub})_1$, $(\phi_{iso})_1$ and $(\phi_{sup})_1$ are the first mode shape of story drifts of the substructure, isolation layer and superstructure, respectively. Using the definitions of Equations (6), (7) and (8) and neglecting the high-order terms of $\omega_{iso}/\omega_{sub}$ and $\omega_{iso}/\omega_{sup}$, the first modal damping ratio ξ_1 can be obtained based on the classical damping assumption in which the off-diagonal terms of the modal damping matrix is neglected

$$\xi_1 = \frac{\xi_{iso}}{\left(1+\dfrac{2(1+r_{sup})}{r_{sub}}\left(\dfrac{\omega_{iso}}{\omega_{sub}}\right)^2+\dfrac{2r_{sup}}{1+r_{sup}}\left(\dfrac{\omega_{iso}}{\omega_{sup}}\right)^2\right)}, \tag{14}$$

and the first modal participation mass ratio L_1 can be determined by

$$L_1 = \frac{r_{sub}+2(r_{sub}+r_{sup}+1)\left(\dfrac{\omega_{iso}}{\omega_{sub}}\right)^2+\dfrac{2r_{sub}r_{sup}}{1+r_{sup}}\left(\dfrac{\omega_{iso}}{\omega_{sup}}\right)^2}{(1+r_{sub}+r_{sup})\left(\dfrac{r_{sub}}{1+r_{sup}}+2\left(\dfrac{\omega_{iso}}{\omega_{sub}}\right)^2+\dfrac{2r_{sub}r_{sup}}{(1+r_{sup})^2}\left(\dfrac{\omega_{iso}}{\omega_{sup}}\right)^2\right)}. \tag{15}$$

From Equation (14), it is seen that the first modal damping ratio may be significantly affected by the masses and stiffnesses of the substructure and superstructure. If the elastic lateral stiffnesses of the substructure and superstructure are much greater than the effective lateral stiffness of the isolation system such that $\omega_{iso}/\omega_{sub}$ and $\omega_{iso}/\omega_{sup}$ are sufficiently small, it is reasonable to assume that the first vibration mode is the isolation mode and the effective damping ratio is equal to the first modal damping ratio.

PARAMETRIC STUDY

Using the above formulated dynamic properties, a series of parametric studies are conducted as follows. Two cases of mass ratios are included with $(r_{sub}, r_{sup})=(1,5)$ and $(r_{sub}, r_{sup})=(2,5)$. The cases with $r_{sub}>r_{sup}$ are excluded because they rarely occur in practice except for the application called the 'mass absorber' [23] or 'building mass damper' [24] which is irrelevant to the seismic isolation technology. The frequency ratios, $\omega_{sub}/\omega_{iso}$ and $\omega_{sup}/\omega_{iso}$, are assumed to vary from 3 to 40. The lower bound of 3 is selected according to IBC2006 [9, 10], where it is specified that the effective period of the isolated structure at the design displacement should be three times greater than the elastic period of the fixed-base superstructure such that the equivalent lateral force procedure is permitted to be applied to the design of seismically base-isolated buildings. On the other hand, the upper bound value of 40 is selected considering that in practice the substructure may be substantially stiffened such that the existing design specifications for base-isolated buildings may be applicable to mid-story isolated buildings. The inherent viscous damping ratio of 5% is assumed for the superstructure and substructure, i.e. $\xi_{sub}=\xi_{sup}=0.05$, whereas the equivalent damping ratio of 20% is presumed for the isolation system, i.e. $\xi_{iso}=0.2$. The effective period of the isolation system is assumed to be 2.0 s or $\omega_{iso}=\pi$.

DOI: 10.1002/eqe

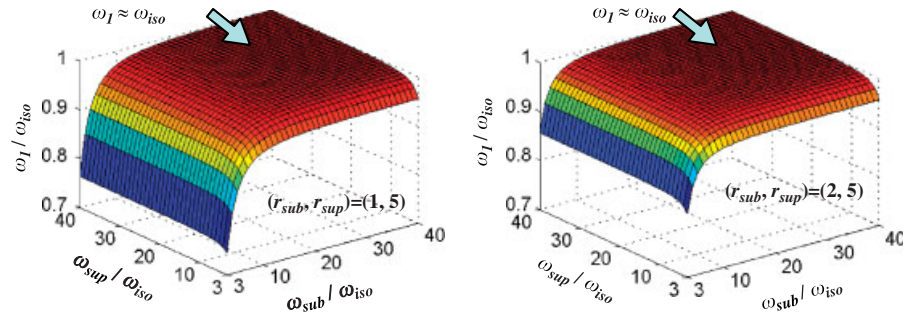

Figure 2. Comparison between fundamental modal frequency and nominal frequency of isolation system with various $\omega_{\text{sub}}/\omega_{\text{iso}}$ and $\omega_{\text{sup}}/\omega_{\text{iso}}$.

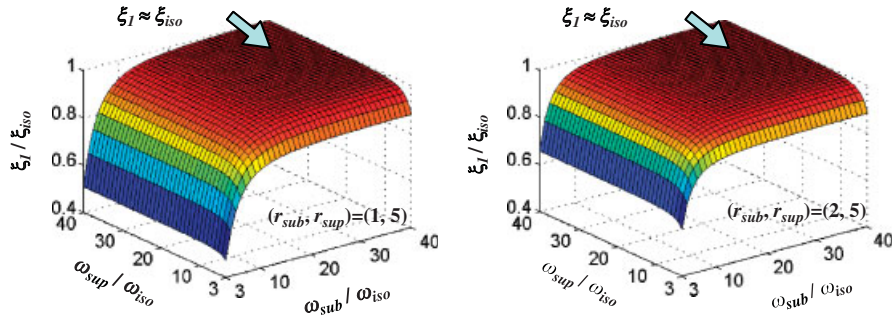

Figure 3. Comparison between first modal damping ratio and equivalent damping ratio of isolation system with various $\omega_{\text{sub}}/\omega_{\text{iso}}$ and $\omega_{\text{sup}}/\omega_{\text{iso}}$.

The comparison between the fundamental modal natural frequency ω_1 and the nominal frequency of the isolation system ω_{iso} with respect to various frequency ratios $\omega_{\text{sub}}/\omega_{\text{iso}}$ and $\omega_{\text{sup}}/\omega_{\text{iso}}$ is shown in Figure 2. From the figure, it is seen that to assume $\omega_1 \approx \omega_{\text{iso}}$ is reasonable when both the nominal frequencies of the substructure and superstructure are much higher than the nominal frequency of the isolation system. In addition, it is obvious from the figure that $\omega_{\text{sub}}/\omega_{\text{iso}}$ has a more significant influence than $\omega_{\text{sup}}/\omega_{\text{iso}}$ on the first modal frequency. Based on the classical damping assumption, the first modal damping ratio ξ_1 and the first modal participation mass ratio L_1 varying with respect to $\omega_{\text{sub}}/\omega_{\text{iso}}$ and $\omega_{\text{sup}}/\omega_{\text{iso}}$ are illustrated in Figures 3 and 4, respectively. From Figure 3, it is seen that the first modal damping ratio is proportional to $\omega_{\text{sub}}/\omega_{\text{iso}}$, $\omega_{\text{sup}}/\omega_{\text{iso}}$ and r_{sub} and gradually approaches the equivalent damping ratio of the isolation system ξ_{iso} when $\omega_{\text{sub}}/\omega_{\text{iso}}$ and $\omega_{\text{sup}}/\omega_{\text{iso}}$ become larger. However, for larger $\omega_{\text{sub}}/\omega_{\text{iso}}$ and $\omega_{\text{sup}}/\omega_{\text{iso}}$, the effect of r_{sub} becomes less significant. Furthermore, $\omega_{\text{sub}}/\omega_{\text{iso}}$ has a more significant influence than $\omega_{\text{sup}}/\omega_{\text{iso}}$ on the first modal damping ratio. It can be proved from Equation (14) that since $2(1+r_{\text{sup}})/r_{\text{sub}} \geqslant 2r_{\text{sup}}/(1+r_{\text{sup}})$ always holds if $r_{\text{sub}} < r_{\text{sup}}$ ($r_{\text{sub}} > 0$ and $r_{\text{sup}} > 0$), $(\omega_{\text{iso}}/\omega_{\text{sub}})^2$ has the more significant weighting factor than $(\omega_{\text{iso}}/\omega_{\text{sub}})^2$. From the above observations, it can be concluded that the lateral stiffness of the substructure is an important parameter affecting the equivalent damping ratio of a mid-story isolated building. Besides, assuming that the behavior of the superstructure as a rigid body in the simplified two-lumped-mass structural model may result into overestimates of the first modal frequency and the first modal damping ratio. In order to demonstrate the validity of the modal analysis under the classical damping assumption, the difference between the first modal damping ratio calculated under decoupling approximation and that calculated by the state space method [25, 26] is presented in Figure 4 in which '*Error*' is defined as

$$\left| \frac{\text{1st modal damping (non-classical damping)} - \text{1st modal damping (classical damping)}}{\text{1st modal damping (non-classical damping)}} \right| \times 100\%. \tag{16}$$

DOI: 10.1002/eqe

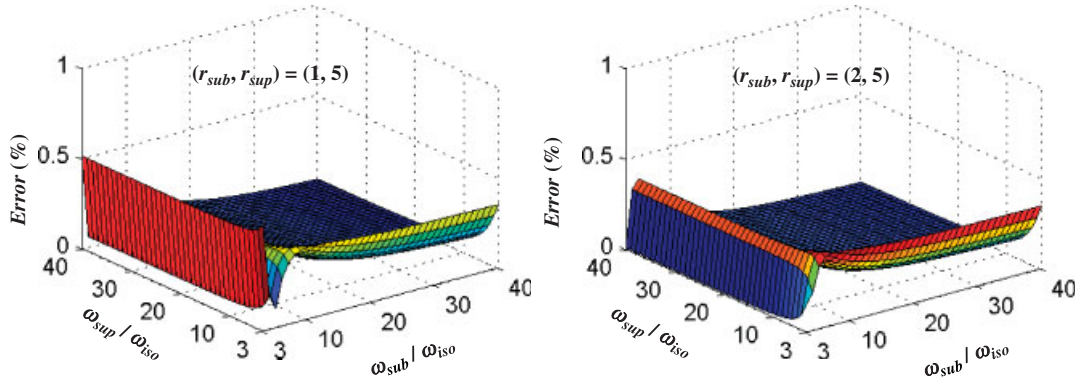

Figure 4. Error in first modal damping ratio introduced by diagonalization procedure with various $\omega_{\text{sub}}/\omega_{\text{iso}}$ and $\omega_{\text{sup}}/\omega_{\text{iso}}$.

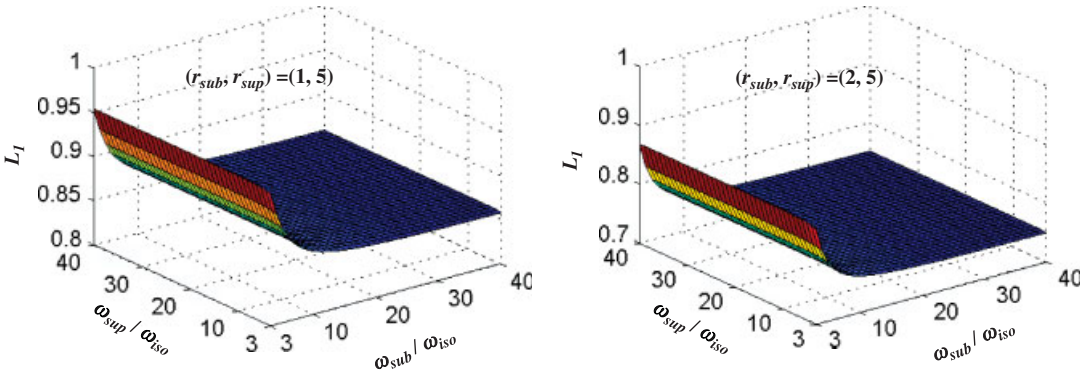

Figure 5. First modal participation mass ratio with various $\omega_{\text{sub}}/\omega_{\text{iso}}$ and $\omega_{\text{sup}}/\omega_{\text{iso}}$.

It can be seen from Figure 4 that the error in the first damping ratio introduced by diagonalization procedure is very limited and acceptable in the considered mass ratio cases and frequency ratio ranges (i.e. *Error* is less than 0.5%). As depicted in Figure 5, the increases in r_{sub} and $\omega_{\text{sub}}/\omega_{\text{iso}}$ result in the reduction of the first modal participation mass ratio L_1. $\omega_{\text{sub}}/\omega_{\text{iso}}$ has a more significant effect than $\omega_{\text{sup}}/\omega_{\text{iso}}$ on the first modal participation mass ratio. It can be proved from Equation (15) that since $2(r_{\text{sub}}+r_{\text{sup}}+1)>2r_{\text{sub}}r_{\text{sup}}/(1+r_{\text{sup}})>2r_{\text{sub}}r_{\text{sup}}/(1+r_{\text{sup}})^2$ always holds if $r_{\text{sub}}<r_{\text{sup}}$ ($r_{\text{sub}}>0$ and $r_{\text{sup}}>0$), the weighting factors to $(\omega_{\text{iso}}/\omega_{\text{sub}})^2$ are larger than those to $(\omega_{\text{iso}}/\omega_{\text{sup}})^2$. Furthermore, the first modal participation mass ratio becomes nearly a constant when $\omega_{\text{sub}}/\omega_{\text{iso}}$ is larger. In summary, the important system characteristics of a mid-story isolated building, including the fundamental modal frequency ω_1, the first modal damping ratio ξ_1 and the first modal participation mass ratio L_1, are more significantly affected by both the stiffness and mass of the substructure than by those of the superstructure. The assumptions that $\omega_1=\omega_{\text{iso}}$ and $\xi_1=\xi_{\text{iso}}$ are rational or acceptable when $\omega_{\text{sub}}/\omega_{\text{iso}}$ is sufficiently large.

The dynamic characteristics of the higher modes varying corresponding to $\omega_{\text{sub}}/\omega_{\text{iso}}$ and $\omega_{\text{sup}}/\omega_{\text{iso}}$ are summarized in Figures 6 and 7. From Figures 6(a) and (b), it is seen that the third modal participation mass ratio is nearly zero in the frequency ratio region where the second modal participation mass ratio is effective and vice versa. In between the two frequency ratio regions where either the second or the third mode is effective, there exists a frequency ratio bandwidth in which the coupling of higher modes occurs [19, 20]. Outside the modal coupling zone, the effective higher mode will be either the second mode or the third mode depending on $\omega_{\text{sub}}/\omega_{\text{iso}}$ and $\omega_{\text{sup}}/\omega_{\text{iso}}$. The two higher modes generally are not effective simultaneously. Besides, as shown in Figures 7(a) and (b), corresponding to the effective higher mode categorized in Figure 6, the modal natural frequency nearly coincides with the nominal frequency of the substructure ω_{sub}, i.e.

DOI: 10.1002/eqe

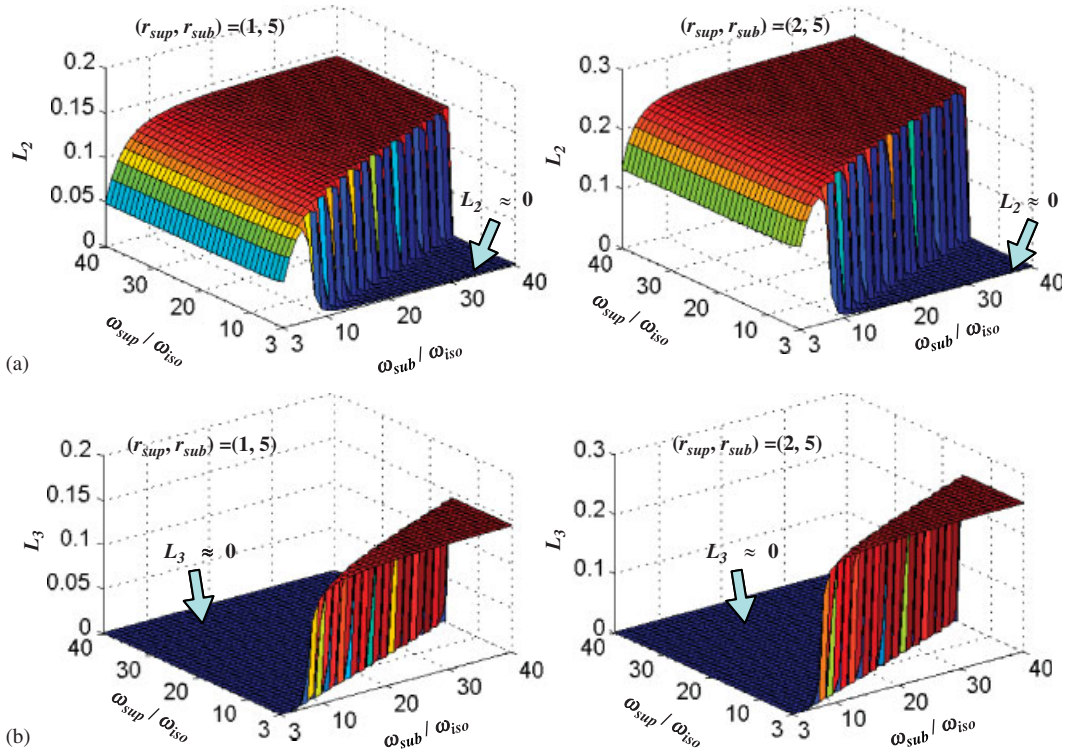

Figure 6. Higher modal participation mass ratios with various $\omega_{sub}/\omega_{iso}$ and $\omega_{sup}/\omega_{iso}$: (a) Second modal participation mass ratio and (b) third modal participation mass ratio.

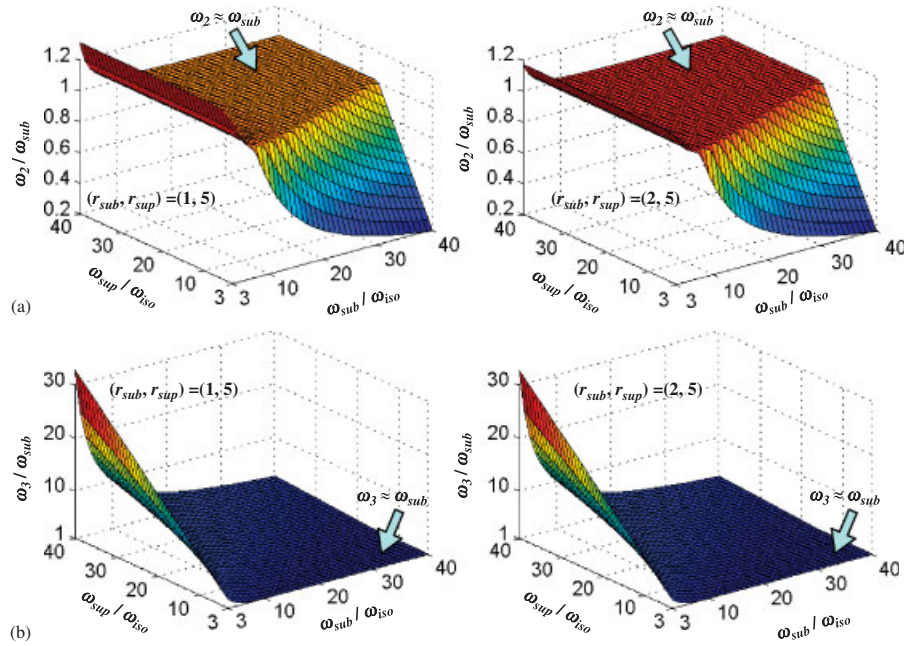

Figure 7. Comparison between higher modal natural frequencies and nominal frequency of substructure with various $\omega_{sub}/\omega_{iso}$ and $\omega_{sup}/\omega_{iso}$: (a) Second modal naural frequency and (b) third modal natural frequency.

DOI: 10.1002/eqe

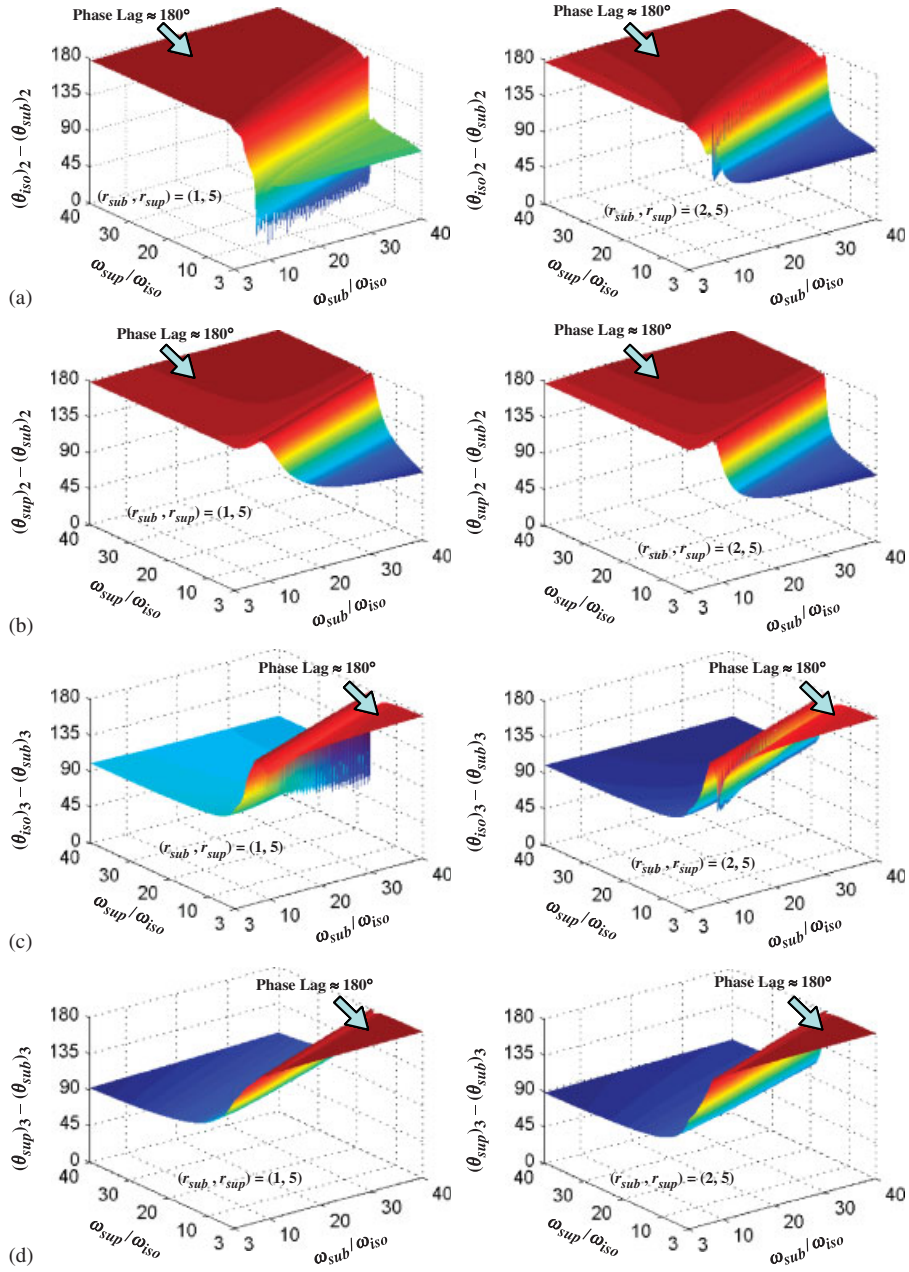

Figure 8. Phase lags of higher modes with various $\omega_{sub}/\omega_{iso}$ and $\omega_{sup}/\omega_{iso}$: (a) Phase lag of super-floor relative to substructure in second mode shape; (b) phase lag of superstructure relative to substructure in second mode shape; (c) phase lag of super-floor relative to substructure in third mode shape; and (d) phase lag of superstructure relative to substructure in third mode shape.

$\omega_2 \approx \omega_{sub}$ or $\omega_3 \approx \omega_{sub}$. Using the non-proportional damping theory and solving Equation (9) by the state space method [25, 26], the components of the nth mode shape of story drifts are written in a complex form as follows:

$$\{\phi_n\} = \begin{Bmatrix} (\phi_{sub})_n \\ (\phi_{iso})_n \\ (\phi_{sup})_n \end{Bmatrix} = \begin{Bmatrix} (\mathrm{Re}_{sub})_n + i(\mathrm{Im}_{sub})_n \\ (\mathrm{Re}_{iso})_n + i(\mathrm{Im}_{iso})_n \\ (\mathrm{Re}_{sup})_n + i(\mathrm{Im}_{sup})_n \end{Bmatrix} = \begin{Bmatrix} (A_{sub})_n \, e^{i(\theta_{sub})_n} \\ (A_{iso})_n \, e^{i(\theta_{iso})_n} \\ (A_{sup})_n \, e^{i(\theta_{sup})_n} \end{Bmatrix} \quad (n = 1, 2, 3), \tag{17}$$

DOI: 10.1002/eqe

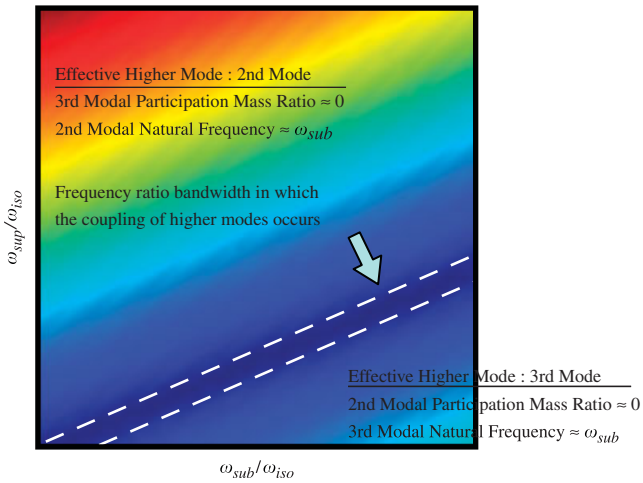

Figure 9. Summarized dynamic characteristics of higher modes.

where $(\mathrm{Re_{sub}})_n$ and $(\mathrm{Im_{sub}})_n$ are the real and imaginary parts of $(\phi_{\mathrm{sub}})_n$, respectively; $(\mathrm{Re_{iso}})_n$ and $(\mathrm{Im_{iso}})_n$ are the real and imaginary parts of $(\phi_{\mathrm{iso}})_n$, respectively; $(\mathrm{Re_{sup}})_n$ and $(\mathrm{Im_{sup}})_n$ are the real and imaginary parts of $(\phi_{\mathrm{sup}})_n$, respectively; $(A_{\mathrm{sub}})_n$, $(A_{\mathrm{iso}})_n$ and $(A_{\mathrm{sup}})_n$ are the amplitudes of the story drifts of the substructure, isolation layer and superstructure, respectively; $(\theta_{\mathrm{sub}})_n$, $(\theta_{\mathrm{iso}})_n$ and $(\theta_{\mathrm{sup}})_n$ are the phase angles of the story drifts of the substructure, isolation layer and superstructure, respectively, corresponding to the nth vibration mode. The phase lags of the isolation layer and superstructure relative to the substructure of the second and third mode shapes are, respectively, denoted as $(\theta_{\mathrm{iso}})_2-(\theta_{\mathrm{sub}})_2$, $(\theta_{\mathrm{sup}})_2-(\theta_{\mathrm{sub}})_2$, $(\theta_{\mathrm{iso}})_3-(\theta_{\mathrm{sub}})_3$ and $(\theta_{\mathrm{sup}})_3-(\theta_{\mathrm{sub}})_3$. As shown in Figures 8(a)–(d), these phase lags almost equal to 180° corresponding to the effective higher mode shapes. Therefore, in the effective higher mode, the substructure always displaces in the direction opposite to the isolation layer and superstructure. In summary, the dynamic characteristics of higher modes can be categorized in Figure 9 in which the domain formed corresponding to various frequency ratios $\omega_{\mathrm{sub}}/\omega_{\mathrm{iso}}$ and $\omega_{\mathrm{sup}}/\omega_{\mathrm{iso}}$ is divided into three regions (1) the second mode effective region, (2) the third mode effective region and (3) the bandwidth of modal coupling [19, 20].

RESPONSE SPECTRUM ANALYSIS

The validity of the response spectrum analysis under decoupling approximation has been demonstrated in the previous researches [27, 28]. Therefore, in addition to the parametric study on the dynamic characteristics of the assumed three-lumped mass model, the seismic responses are calculated using the response spectrum analysis. The complete quadratic combination (CQC) method is used to estimate the maximum responses from each modal peak spectral value [29]. The 5% damped design spectrum with the spectral response acceleration parameters of $S_{DS}=0.8$ and $S_{D1}=0.4$ is selected for the study, as illustrated in Figure 10. The design spectrum is modified by damping adjustment factors [9–11] corresponding to the modal damping ratios of different modes.

The maximum inertial forces and base shear force acting at the substructure are summarized in Figure 11. The second modal, third modal and the maximum inertia forces at the substructure,$(F_{\mathrm{sub}})_2$,$(F_{\mathrm{sub}})_3$ and F_{sub}, are shown in Figures 11(a)–(c), respectively. From the comparison of these three figures, it is interesting to find that the maximum inertia force exerting at the substructure of Figure 11(c) is almost equal to the maximum modal inertia force of either the second or the third mode of Figure 11(a) or (b). Therefore, it is concluded that the maximum inertia force exerting at the substructure is primarily attributed to the higher modal responses rather than the fundamental modal response. Besides, recognizing that m_{sub} corresponding to $r_{\mathrm{sub}}=2$ is two times of m_{sub} of $r_{\mathrm{sub}}=1$, a larger r_{sub} generally results in a larger maximum inertia force

DOI: 10.1002/eqe

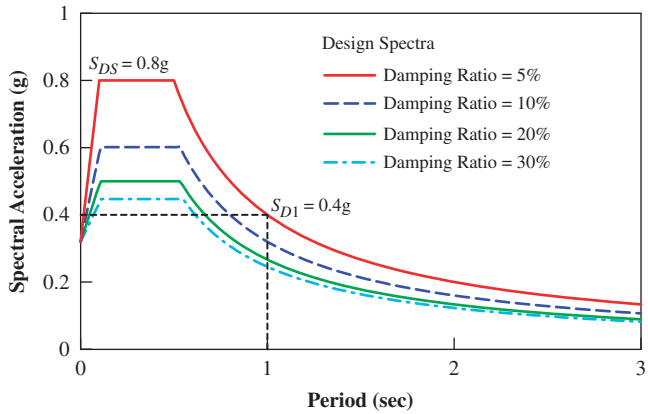

Figure 10. Design spectrum adopted in response spectrum analysis.

F_{sub} acting at the sub-floor (or substructure) below the isolation system as shown in Figure 11(c). Similarly, a larger r_{sub} also deduces a larger maximum base shear force V_{sub} as shown in Figure 11(d). Furthermore, from the comparison between Figures 11(c) and (d), it is apparent that the maximum inertia force acting at the sub-floor due to higher mode responses has contributed significantly to the maximum base shear force. Therefore, the calculation of design force of the substructure (or the base shear force) should carefully consider the contribution of higher mode responses. Since the lateral force distribution of the equivalent lateral force design procedure for base-isolated buildings is primarily deduced from the fundamental modal response as given in the design code [9–11], the findings of this study will generally introduce difficulties in establishing an appropriate equivalent lateral force design procedure for mid-story isolated buildings.

The first modal and maximum inertial forces, respectively, exerting at the super-floor and superstructure, denoted as $(F_{iso})_1$, F_{iso}, $(F_{sup})_1$ and F_{sup}, are summarized in Figures 12(a)–(d). The maximum inertia forces acting at the super-floor and superstructure are mainly attributed to the first modal inertial forces as can be realized from the comparison between Figures 12(a) and (b) as well as Figures 12(c) and (d). However, it should be noted that significant response amplifications of these maximum inertia forces are seen in the figures when $\omega_{sub}/\omega_{iso}$ and $\omega_{sup}/\omega_{iso}$ fall within the frequency ratio bandwidth in which the coupling of higher modes occurs. This response amplification due to modal coupling is particularly obvious when $\omega_{sub}/\omega_{iso}$ and $\omega_{sup}/\omega_{iso}$ are relatively small. This phenomenon cannot be reflected based on the simplified two-lumped-mass structural model. From the comparison of Figures 11(c), 12(b) and (d), the maximum inertia forces at the super-floor and superstructure are not as sensitive as the maximum inertia force at the substructure to the variations of $\omega_{sub}/\omega_{iso}$ and r_{sub}. In addition, it is also realized that since the accelerations corresponding to the maximum inertia forces acting at the super-floor and superstructure of Figures 12(b) and (d) are much smaller than the accelerations with respect to the maximum inertia forces acting at the sub-floor of Figure 11(c), the maximum acceleration transmitted to the superstructure is effectively reduced similar to that of a base-isolated structure if $\omega_{sub}/\omega_{iso}$ is within the frequency range considered in this study.

The analytical study discloses that the effect of the substructure on the seismic responses of mid-story isolated buildings is of particular importance when the substructure possesses a relatively small nominal frequency ω_{sub}. It is obvious that designing the substructure and superstructure with higher nominal frequencies, ω_{sub} and ω_{sup}, will produce a better seismic performance of the superstructure. The adoption of the proposed formulas given in Equations (14) and (15) together with the observations from the aforementioned analytical study may be helpful for the appropriate design of the substructure and superstructure. Furthermore, the participation of higher mode responses should be appropriately taken into account when designing the substructure. When the substructure possesses a larger mass, the modal participation mass ratio of higher modes becomes larger. Therefore, the effects of higher modes should be appropriately considered when designing the substructure using the equivalent lateral force procedure for mid-story isolated buildings.

DOI: 10.1002/eqe

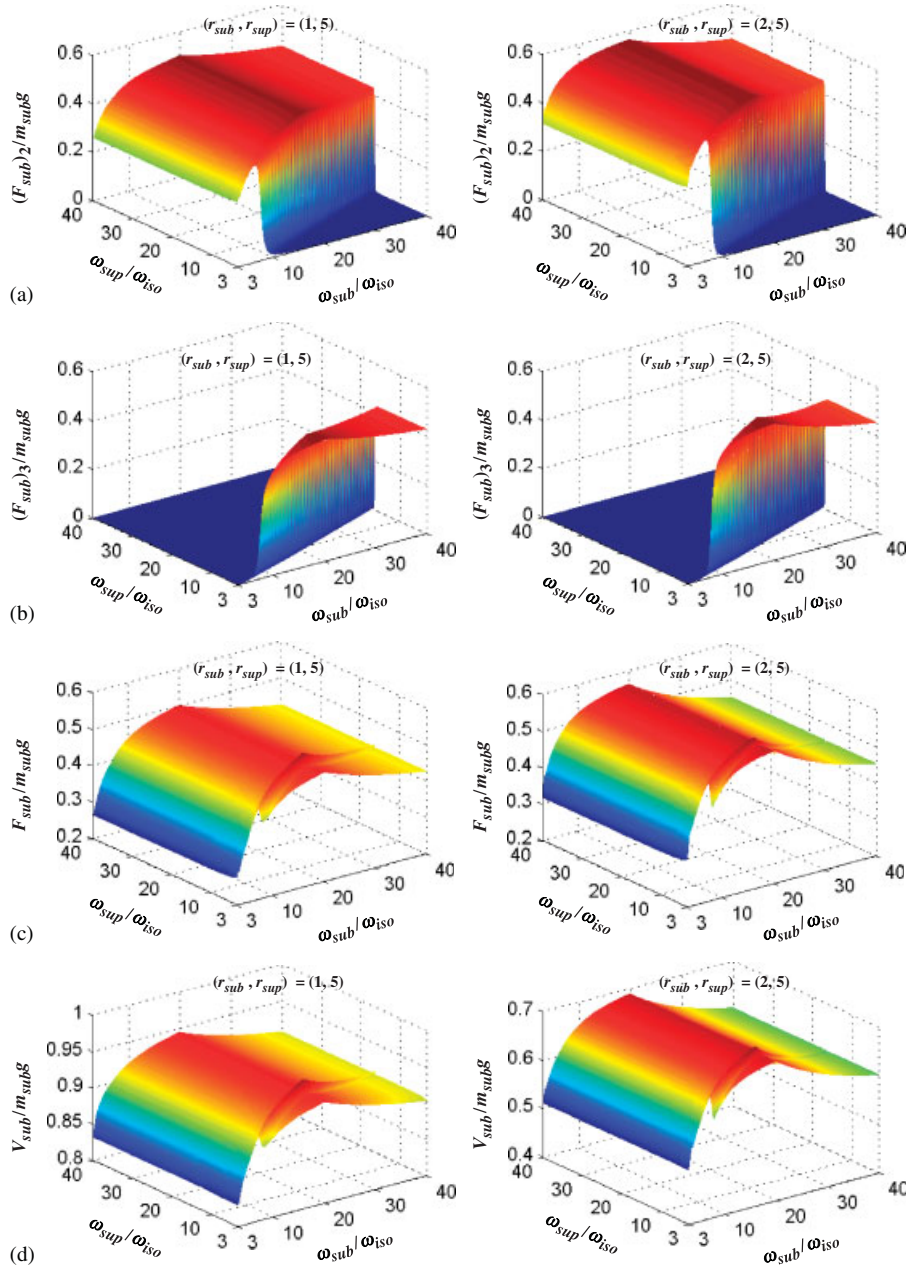

Figure 11. Force responses at substructure with various $\omega_{sub}/\omega_{iso}$ and $\omega_{sup}/\omega_{iso}$: (a) Second modal inertia force at substructure; (b) third modal inertia force at substructure; (c) maximum inertia force at substructure; and (d) maximum story shear at substructure.

CONCLUSIONS

The equivalent linear characteristics of mid-story isolated buildings represented by a three-lumped-mass model are formulated. On the basis of the parametric study, it is found that the two frequency ratios, $\omega_{sub}/\omega_{iso}$ and $\omega_{sup}/\omega_{iso}$, have significant influences on the first modal frequency, first modal damping ratio and first modal participation mass ratio. The isolation frequency and equivalent damping ratio are, respectively, equal to the first modal frequency and first damping ratio if both the nominal frequencies of the substructure and superstructure are much higher than that of the isolation system. Furthermore, since the effect of $\omega_{sub}/\omega_{iso}$ is more significant, the mass and

DOI: 10.1002/eqe

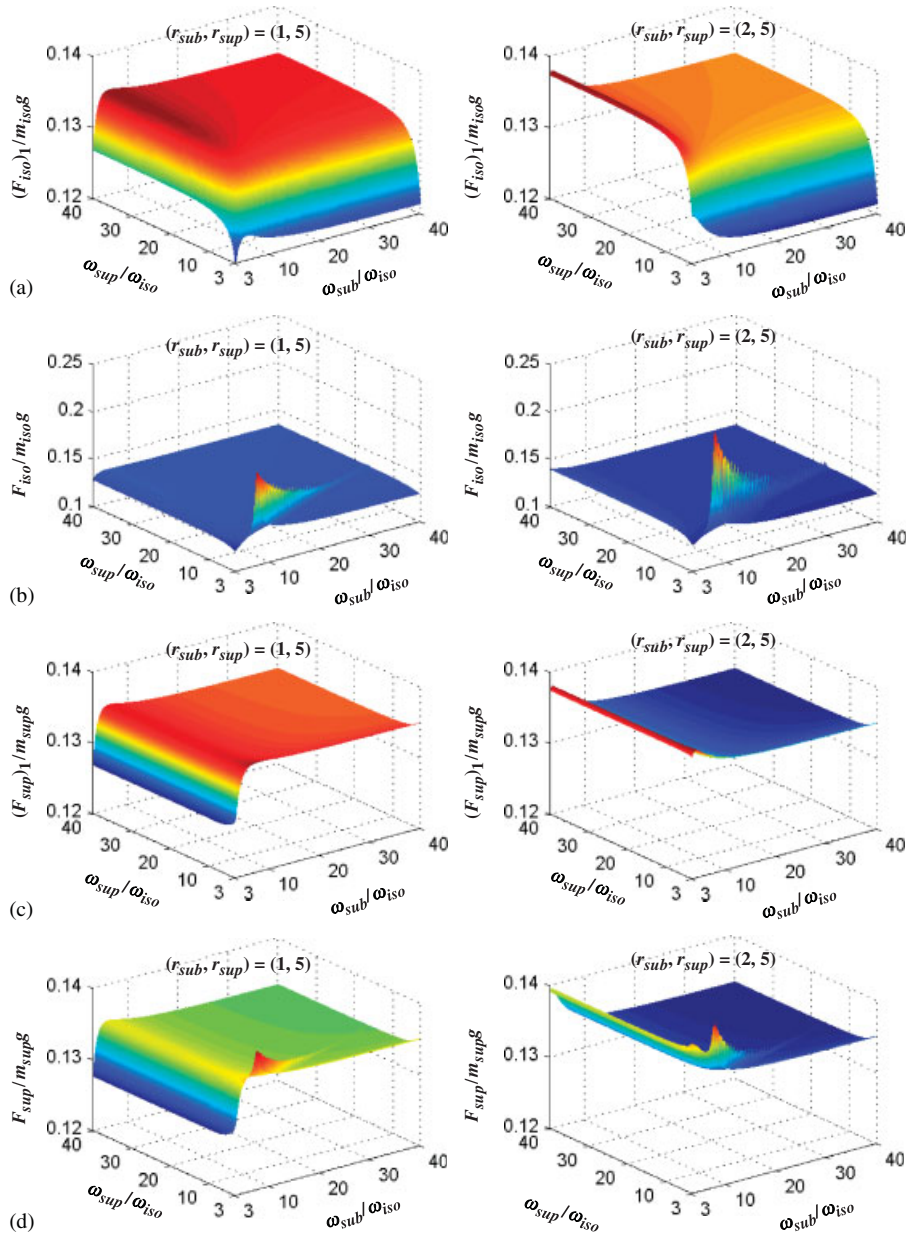

Figure 12. Force responses at super-floor and superstructure with various $\omega_{sub}/\omega_{iso}$ and $\omega_{sup}/\omega_{iso}$: (a) First modal inertia force at super-floor; (b) maximum inertia force at super-floor; (c) first modal inertia force at superstructure; and (d) maximum inertia force at superstructure.

stiffness of the substructure are more important than those of the superstructure in affecting the dynamic characteristics of a mid-story isolated building. With regard to higher modes, outside the frequency ratio bandwidth in which the coupling of higher modes occurs, the effective higher mode is either the second mode or the third mode depending on $\omega_{sub}/\omega_{iso}$ and $\omega_{sup}/\omega_{iso}$. Observed from the response spectrum analysis, the maximum inertia forces acting at the super-floor and superstructure are mainly attributed to the first modal inertial forces. However, it should be noted that significant response amplifications of these maximum inertia forces may occur when $\omega_{sub}/\omega_{iso}$ and $\omega_{sup}/\omega_{iso}$ fall within the frequency ratio bandwidth of the coupling of higher modes. Besides, it is important to note that the contribution of higher mode responses to the inertia force acting at the substructure is significant such that the design of substructure should carefully consider the

DOI: 10.1002/eqe

higher mode contribution. Consequently, the lateral force distribution often used in the equivalent lateral force procedure specified in the design code for conventional base-isolated buildings may not be applicable to mid-story isolated buildings without appropriately considering the effect of higher modes.

ACKNOWLEDGEMENTS

The study was supported by the National Center for Research on Earthquake Engineering of Taiwan. The support is acknowledged.

REFERENCES

1. Elsesser E, Jokerst M, Naaseh S. Historic upgrades in San Francisco. *Civil Engineering* (ASCE) 1997; **67**(10): 50–53.
2. Nagarajaiah S, Xiaohong S. Response of base-isolated USC hospital building in Northridge earthquake. *Journal of Structural Engineering* (ASCE) 2000; **126**:1177–1186.
3. Fujita T. Seismic isolation of civil buildings in Japan. *Progress in Structural Engineering and Materials* 1998; **1**(3):295–300.
4. Kamada T, Fujita T. Current status of seismic isolation and vibration control to buildings, cultural heritage and industrial facilities in Japan. *Proceedings of the 10th World Conference on Seismic Isolation*, *Energy Dissipation and Active Vibrations Control of Structures*, Istanbul, 2007.
5. Zhou FL, Xian QL, Tan P, Cui J, Huan XY. Current status of application, R&D and design rules for seismic isolation, energy dissipation and structural control of buildings, bridges and viaducts and cultural heritage in the P. R. China. *Proceedings of the 10th World Conference on Seismic Isolation*, *Energy Dissipation and Active Vibrations Control of Structures*, Istanbul, 2007.
6. Whittaker D, Robinson WH. Progress of application and Research & Development for seismic isolation and passive energy dissipation for civil and industrial structures in New Zealand. *Proceedings of the 10th World Conference on Seismic Isolation*, *Energy Dissipation and Active Vibrations Control of Structures*, Istanbul, 2007.
7. Chang KC, Hwang JS, Chan TC, Tau CC, Wang SJ. Application, R&D and design rules for seismic isolation and energy dissipation systems for buildings and bridges in Taiwan. *Proceedings of the 10th World Conference on Seismic Isolation*, *Energy Dissipation and Active Vibrations Control of Structures*, Istanbul, 2007.
8. Federal Emergency Management Agency FEMA450. *NEHRP Recommended Provisions for Seismic Regulations for New Buildings and other Structures*. Building Seismic Safety Council: Washington, DC, 2003.
9. International Code Council. *International Building Code*. ICC: Whittier, CA, 2006.
10. ASCE Standard ASCE/SEI 7-05. *Minimum Design Loads for Building and Other Structures*. American Society of Civil Engineers: New York, 2006.
11. *Seismic Design Code for Buildings*. Ministry of Interior: Taipei, Taiwan, 2006.
12. Ogura K, Takayama M, Tsujita O, Kimura Y, Wada A. Seismic response of mid-story isolated buildings. *Journal of Structural and Construction Engineering*, *Architectural Institute of Japan* 1999; **516**:99–104.
13. Xu ZG, Hu MY, Zhou FL. Discuss on mid-story isolation of building. *Earthquake Resistant Engineering and Retrofitting* 2004; **5**:23–28.
14. Koh T, Kobayashi M. Vibratory characteristics and earthquake response of mid-story isolated buildings. *Memoirs of the Institute of Sciences and Technology*, *Meiji University* 2000; **39**(12):97–114.
15. Li XZ, Ou HL, Lin S. Simplified analysis on calculation model of interlayer seismic isolation. *Earthquake Engineering and Engineering Vibration* 2002; **22**(1):121–125.
16. Murakami K, Kitamura H, Matsushima Y. The prediction for seismic responses of the two-mass model with the mid-story isolation system. *Journal of Structural and Construction Engineering. Architectural Institute of Japan* 2001; **549**:51–58.
17. Kobayashi M, Koh T. Earthquake response prediction and aseismic performance of mid-story isolated system. *Journal of Structural and Construction Engineering*, *Architectural Institute of Japan* 2002; **558**:109–116.
18. Tsai IC. *Analytical Studies on Seismic Isolation Design Codes for Buildings and Bridges in Taiwan. Research Report of Center for Earthquake Engineering Research*, National Taiwan University, 2002.
19. Koh T, Kobayashi M. Analytical study of modal coupling effect on mid-story isolation system by eigen value analysis and random vibration analysis. *Summaries of Technical Papers of Annual Meeting*, *Architectural Institute of Japan. B-2*, *Structures II*, *Structural Dynamics Nuclear Power Plants*, Architectural Institute of Japan, 2004; 333–334.
20. Chang KC, Hwang JS, Wang SJ, Lee BH, Lin MH, Chiang CC. Analytical and experimental studies on seismic behavior of buildings with mid-story isolation. *Proceedings of the 10th International Conference on Structural Safety and Reliability*, Osaka, 2009.
21. Kelly JM. Base isolation: Linear theory and design. *Earthquake Spectra* 1990; **6**(2):223–244.
22. Kelly JM. *Earthquake-Resistant Design with Rubber* (2nd edn). Springer: London, 1996.
23. Villaverde R, Mosqueda G. Aseismic roof isolation system: Analytical and shake table studies. *Earthquake Engineering and Structural Dynamics* 1999; **28**(3):217–234.

DOI: 10.1002/eqe

24. Otsuka H, Marukawa R, Ehara E, Kimizuka M, Ishigaki H. Design for BMD (building mass damper) structure. *Journal of Constructional Steel* 2000; **8**:149–156.
25. Hwang JS, Chang KC, Tsai MH. Composite damping ratio of seismically isolated regular bridges. *Engineering Structures* 1997; **19**(1):55–62.
26. Veletsos AS, Ventura CE. Modal analysis of non-classically damped systems. *Earthquake Engineering and Structural Dynamics* 1986; **14**:217–243.
27. Yang JN, Sarkani S, Long FX. A response spectrum approach for seismic analysis of non-classically damped structures. *Engineering Structures* 1990; **12**:173–184.
28. Warburton GB, Soni SR. Errors in response calculations for non-classically damped structures. *Earthquake Engineering and Structural Dynamics* 1977; **5**:365–376.
29. Wilson EL, Kiureghian AD, Bayo EP. A replacement for the SRSS method in seismic analysis. *Earthquake Engineering and Structural Dynamics* 1981; **9**:187–194.

DOI: 10.1002/eqe